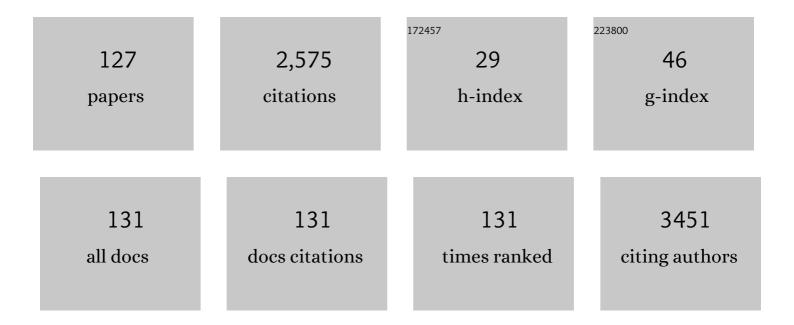
Kwang-Soon Ahn

List of Publications by Year in descending order

Source: https://exaly.com/author-pdf/6262732/publications.pdf Version: 2024-02-01



#	Article	IF	CITATIONS
1	Nickel-foam supported cobalt fluoride hydroxide crystallites as an efficient and durable electrocatalyst for oxygen evolution reaction. Materials Letters, 2022, 308, 131207.	2.6	2
2	Ni ₃ (PO ₄) ₂ Cocatalyst-Supported β–Ga ₂ O ₃ /GaN Photoanodes for Highly Stable Solar Water Splitting. ACS Applied Energy Materials, 2022, 5, 2169-2183.	5.1	6
3	Fabrication and Characterization of the Broccoli-like Structured CuO Thin Films Synthesized by a Facile Hydrothermal Method and Its Photoelectrochemical Water Splitting Application. Metals, 2022, 12, 484.	2.3	2
4	Low-temperature processed nickel oxide hole-transporting layer for perovskite solar cell. Journal of the Korean Physical Society, 2022, 80, 981-985.	0.7	1
5	Semi-Polycrystalline–Polyaniline Empowered Electrochemical Capacitor. Energies, 2022, 15, 2001.	3.1	10
6	Electrochemically co-deposited WO3-V2O5 composites for electrochromic energy storage applications. Electrochimica Acta, 2022, 422, 140340.	5.2	27
7	Effect of molar concentration on the crystallite structures and electrochemical properties of cobalt fluoride hydroxide for hybrid supercapacitors. Electrochimica Acta, 2022, 414, 140203.	5.2	10
8	Amorphous-crystalline dual phase WO3 synthesized by pulsed-voltage electrodeposition and its application to electrochromic devices. Journal of Industrial and Engineering Chemistry, 2021, 94, 264-271.	5.8	36
9	Potentiostatically deposited bimetallic cobalt–nickel selenide nanostructures on nickel foam for highly efficient overall water splitting. International Journal of Hydrogen Energy, 2021, 46, 7297-7308.	7.1	16
10	Multifunctional nitrogen-doped graphene quantum dots incorporated into mesoporous TiO2 films for quantum dot-sensitized solar cells. Journal of Alloys and Compounds, 2021, 870, 159527.	5.5	30
11	Double-layer cobalt selenide/nickel selenide with web-like nanostructures as a high-performance electrode material for supercapacitors. Journal of Electroanalytical Chemistry, 2021, 895, 115479.	3.8	20
12	NiCo-mixed hydroxide nanosheets as a new electrochromic material with fast optical response. Chemical Physics Letters, 2021, 783, 139024.	2.6	3
13	Novel method for synthesis of reduced graphene oxide–Cu2S and its application as a counter electrode in quantum-dot-sensitized solar cells. Applied Surface Science, 2021, 564, 150393.	6.1	11
14	Highly efficient and stable g‑C3N4 decorated Ta3N5 nanotube on n-Si substrate for solar water oxidation. Applied Surface Science, 2021, 565, 150456.	6.1	8
15	Facile Hydrothermal Synthesis and Supercapacitor Performance of Mesoporous Necklace-Type ZnCo2O4 Nanowires. Catalysts, 2021, 11, 1516.	3.5	11
16	Cu3Se2 nanomeshes constructed by enoki-mushroom-like Cu3Se2 and their application to quantum dot-sensitized solar cells. Applied Surface Science, 2020, 499, 143935.	6.1	13
17	Microfluidics-enabled rational design for Ag–ZnO nanocomposite films for enhanced photoelectrochemical performance. CrystEngComm, 2020, 22, 646-653.	2.6	10
18	Self-standing star-shaped tri-metallic oxides for pseudocapacitive energy storage electrode materials. Applied Surface Science, 2020, 530, 147251.	6.1	15

KWANG-SOON AHN

#	Article	IF	CITATIONS
19	Nanoporous Ta ₃ N ₅ <i>via</i> electrochemical anodization followed by nitridation for solar water oxidation. Dalton Transactions, 2020, 49, 15023-15033.	3.3	4
20	Enhanced electrocatalytic activity and electrochemical stability of Cu2S/PbS counter electrode for quantum-dot-sensitized solar cells. Applied Surface Science, 2020, 525, 146643.	6.1	22
21	Visible-light responsive BiNbO ₄ nanosheet photoanodes for stable and efficient solar-driven water oxidation. Physical Chemistry Chemical Physics, 2020, 22, 14042-14051.	2.8	7
22	Color-switchable electrochromic Co(OH)2/Ni(OH)2 nanofilms with ultrafast kinetics for multifunctional smart windows. Nano Energy, 2020, 72, 104720.	16.0	59
23	Functional Blocking Layer of Twisted Tungsten Oxide Nanorod Grown by Electrochemical Anodization for Photoelectrochemical Water Splitting. Journal of the Electrochemical Society, 2020, 167, 066501.	2.9	7
24	Enhanced capacitive performances and excellent stability of cadmium-sulfide-concealed nickel sulfide (Ni3S2/CdS) for electrochemical capacitors. Journal of Alloys and Compounds, 2020, 826, 154211.	5.5	25
25	Electrochemically Deposited Polypyrrole for Counter Electrode of Quasi-Solid-State Dye-Sensitized Solar Cell. Journal of Nanoscience and Nanotechnology, 2020, 20, 546-551.	0.9	6
26	Visible-light photoelectrochemical responses of dye-sensitized, compact TiO ₂ thin films deposited by electron beam evaporation. Molecular Crystals and Liquid Crystals, 2019, 679, 119-126.	0.9	0
27	Potentiostatic deposition of CoNi2Se4 nanostructures on nickel foam as efficient battery-type electrodes for supercapacitors. Journal of Electroanalytical Chemistry, 2019, 850, 113371.	3.8	14
28	Bifunctional NiCo2Se4 and CoNi2Se4 nanostructures: Efficient electrodes for battery-type supercapacitors and electrocatalysts for the oxygen evolution reaction. Journal of Industrial and Engineering Chemistry, 2019, 79, 370-382.	5.8	41
29	Potentiodynamic Electrodeposition of CoSe2 Films and Their Excellent Electrocatalytic Activity as Counter Electrodes for Dye-Sensitized Solar Cells. Journal of the Electrochemical Society, 2019, 166, H473-H479.	2.9	3
30	Multilayered Fluorine Doped SnO2 Inverse Opal/WO3/BiVO4 Film for Solar Water Oxidation: Systematic Development and Defined Role of Each Layer. Journal of the Electrochemical Society, 2019, 166, H750-H763.	2.9	4
31	Oxygen evolution NiOOH catalyst assisted V2O5@BiVO4 inverse opal hetero-structure for solar water oxidation. International Journal of Hydrogen Energy, 2019, 44, 4656-4663.	7.1	28
32	Application of polypyrrole/sodium dodecyl sulfate/carbon nanotube counter electrode for solid-state dye-sensitized solar cells and dye-sensitized solar cells. Chemical Papers, 2019, 73, 2749-2755.	2.2	7
33	Electrolyte effects on undoped and Mo-doped BiVO4 film for photoelectrochemical water splitting. Journal of Electroanalytical Chemistry, 2019, 842, 41-49.	3.8	15
34	Shape Control Iron Pyrite Synthesized by Hot Injection Method: Counter Electrode for Efficient Dye-Sensitized Solar Cells. Electronic Materials Letters, 2019, 15, 350-356.	2.2	5
35	Development of Tungsten Trioxide Using Pulse and Continuous Electrodeposition and Its Properties in Electrochromic Devices. Journal of the Electrochemical Society, 2019, 166, D86-D92.	2.9	26
36	Preparation of nickel selenide by pulsed-voltage electrodeposition and its application as a highly-efficient electrocatalyst at counter electrodes of quantum-dot sensitized solar cells. Electrochimica Acta, 2019, 296, 364-371.	5.2	14

KWANG-SOON AHN

#	Article	IF	CITATIONS
37	Improved electrocatalytic activity of electrodeposited Ni3S4 counter electrodes for dye- and quantum dot-sensitized solar cells. Journal of Industrial and Engineering Chemistry, 2019, 70, 322-329.	5.8	18
38	Facile Electrochemical Synthesis of Manganese Cobalt Sulfide Counter Electrode for Quantum Dot-Sensitized Solar Cells. Journal of the Electrochemical Society, 2018, 165, F375-F380.	2.9	13
39	Rambutan-like cobalt nickel sulfide (CoNi2S4) hierarchitecture for high-performance symmetric aqueous supercapacitors. Journal of Industrial and Engineering Chemistry, 2018, 63, 73-83.	5.8	53
40	Dual roles of a flouride-doped SnO2/TiO2 bilayer based on inverse opal/nanoparticle structure for water oxidation. Journal of the Korean Physical Society, 2018, 72, 260-269.	0.7	3
41	Monolithic Inorganic ZnO/GaN Semiconductors Heterojunction White Light-Emitting Diodes. ACS Applied Materials & Interfaces, 2018, 10, 3761-3768.	8.0	38
42	Tough Hydrogel Electrolytes Doped with Polysulfide Redox Couples for Quantum-dot-sensitized Solar Cells. Chemistry Letters, 2018, 47, 51-54.	1.3	2
43	Vapor-Deposited Tungsten Carbide Nano-Dendrites as Sulfur-Tolerant Electrocatalysts for Quantum Dot-Sensitized Solar Cells. Journal of the Electrochemical Society, 2018, 165, H954-H961.	2.9	0
44	Enhanced electrocatalytic activity and electrochemical stability of copper(I) sulfide electrode electrodeposited on a Ti interlayer-coated fluorine-doped tin oxide substrate and its application to quantum dot-sensitized solar cells. Thin Solid Films, 2018, 660, 46-53.	1.8	5
45	Electrodeposited MoS2 as electrocatalytic counter electrode for quantum dot- and dye-sensitized solar cells. Electrochimica Acta, 2018, 260, 716-725.	5.2	41
46	Annealing effect of fluorine-doped SnO2/WO3 core-shell inverse opal nanoarchitecture for photoelectrochemical water splitting. Journal of the Korean Physical Society, 2017, 70, 162-168.	0.7	6
47	Facile hydrothermal synthesis of cubic spinel AB2O4 type MnFe2O4 nanocrystallites and their electrochemical performance. Applied Surface Science, 2017, 413, 83-91.	6.1	77
48	Revealing the Beneficial Effects of FeVO ₄ Nanoshell Layer on the BiVO ₄ Inverse Opal Core Layer for Photoelectrochemical Water Oxidation. Journal of Physical Chemistry C, 2017, 121, 7625-7634.	3.1	50
49	Facile hydrothermal synthesis and electrochemical supercapacitor performance of hierarchical coral-like ZnCo2O4 nanowires. Journal of Electroanalytical Chemistry, 2017, 785, 48-57.	3.8	85
50	Effect of Lil/I ₂ concentration and photoelectrode thickness on the photovoltaic properties of NiO-based p-type dye-sensitized solar cells. Molecular Crystals and Liquid Crystals, 2017, 653, 99-108.	0.9	1
51	Temperature-dependent DC characteristics of AlInN/GaN high-electron-mobility transistors. Electronic Materials Letters, 2017, 13, 302-306.	2.2	2
52	Enhanced Electrocatalytic Activity of Cu2S-Polyaniline Heterostructure Counter Electrode for Quantum Dot-Sensitized Solar Cells. Journal of the Electrochemical Society, 2017, 164, F1211-F1215.	2.9	8
53	Graphene coated alumina-modified polypyrrole composite films as an efficient Pt-free counter electrode for dye-sensitized solar cells. Electrochimica Acta, 2016, 205, 170-177.	5.2	21
54	Enhanced electrocatalytic activity of electrodeposited F-doped SnO2/Cu2S electrodes for quantum dot-sensitized solar cells. Journal of Power Sources, 2016, 316, 53-59.	7.8	24

#	Article	IF	CITATIONS
55	Cubic Spinel AB ₂ O ₄ Type Porous ZnCo ₂ O ₄ Microspheres: Facile Hydrothermal Synthesis and Their Electrochemical Performances in Pseudocapacitor. Journal of the Electrochemical Society, 2016, 163, A2418-A2427.	2.9	50
56	ZnO transparent conductive electrodes embedded with Pt nanoclusters for high-efficiency GaN-based light-emitting diodes. Journal of the Korean Physical Society, 2016, 68, 274-278.	0.7	3
57	Enhanced performance of reversely transferred, doubly open-ended TiO2 nanotube arrays for front-illuminated dye-sensitized solar cells. Journal of the Korean Physical Society, 2016, 68, 296-301.	0.7	0
58	One-Step Electrodeposited Nickel Cobalt Sulfide Electrocatalyst for Quantum Dot-Sensitized Solar Cells. Journal of the Electrochemical Society, 2016, 163, D175-D178.	2.9	12
59	Beneficial surface passivation of hydrothermally grown TiO2 nanowires for solar water oxidation. Applied Surface Science, 2016, 366, 561-566.	6.1	18
60	Role of WO ₃ Layers Electrodeposited on SnO ₂ Inverse Opal Skeletons in Photoelectrochemical Water Splitting. Journal of Physical Chemistry C, 2016, 120, 5906-5915.	3.1	51
61	Enhanced Efficiency of Nanoporous-layer-covered TiO2 NanotubeArrays for Front Illuminated Dye-sensitized Solar Cells. Journal of Electrochemical Science and Technology, 2016, 7, 52-57.	2.2	0
62	Enhanced Efficiency of Nanoporous-layer-covered TiO ₂ NanotubeArrays for Front Illuminated Dye-sensitized Solar Cells. Journal of Electrochemical Science and Technology, 2016, 7, 52-57.	2.2	1
63	Visible Light Absorbing TiO ₂ Nanotube Arrays by Sulfur Treatment for Photoelectrochemical Water Splitting. Journal of Physical Chemistry C, 2015, 119, 13375-13383.	3.1	79
64	Reactively sputtered nickel nitride as electrocatalytic counter electrode for dye- and quantum dot-sensitized solar cells. Scientific Reports, 2015, 5, 10450.	3.3	78
65	Polypyrrole and Polypyrrole-Multi Wall Carbon Nanotube for Alternative Counter Electrodes in Dye-sensitized Solar Cells. Molecular Crystals and Liquid Crystals, 2015, 620, 71-77.	0.9	4
66	Tungsten trioxide nanorods on flexible carbon cloth for photoelectrochemical water splitting. Materials Letters, 2015, 151, 28-30.	2.6	11
67	Joint Effects of Photoactive TiO ₂ and Fluoride-Doping on SnO ₂ Inverse Opal Nanoarchitecture for Solar Water Splitting. ACS Applied Materials & Interfaces, 2015, 7, 20292-20303.	8.0	72
68	Effect of copper phthalocyanine (CuPc) interlayer on the electrical characteristics of Au/n-GaN Schottky rectifier. Materials Science in Semiconductor Processing, 2015, 30, 420-428.	4.0	10
69	Aggregation control of organic sensitizers for panchromatic dye co-sensitized solar cells. Japanese Journal of Applied Physics, 2014, 53, 08NC04.	1.5	7
70	CdSe Quantum Dot-sensitized, Nanoporous p-type NiO Photocathodes for Quantum Dot-sensitized Solar Cells. Molecular Crystals and Liquid Crystals, 2014, 598, 154-162.	0.9	8
71	Enhanced photoelectrochemical response of CdSe quantum dot-sensitized p-type NiO photocathodes. Physica Status Solidi (A) Applications and Materials Science, 2014, 211, 1868-1872.	1.8	22
72	Dye-Sensitized Solar Cells Composed of Well-Aligned ZnO Nanorod Array Grown with Chemical Bath Deposition Method as the Photo-Electrode. Molecular Crystals and Liquid Crystals, 2014, 597, 120-127.	0.9	2

#	Article	IF	CITATIONS
73	Enhanced Light Harvesting and Electron Lifetime of Front Side-illuminated CdSe Quantum Dot-assembled TiO ₂ Nanotube Arrays for Quantum Dot-sensitized Solar Cells. Molecular Crystals and Liquid Crystals, 2014, 598, 144-153.	0.9	2
74	Bifunctional Effects of CdSe Quantum Dots and Nb2O5 Interlayer for ZnO Nanorods-based Photoelectrochemical Water-Splitting Cells. Electrochimica Acta, 2014, 133, 262-267.	5.2	18
75	Carrier transport mechanism of Mo contact to amorphous hafnium indium zinc oxides. Physica Status Solidi (A) Applications and Materials Science, 2014, 211, 1818-1821.	1.8	1
76	Enhanced electrocatalytic activity of the Au-electrodeposited Pt nanoparticles-coated conducting oxide for the quantum dot-sensitized solar cells. Applied Physics Letters, 2014, 105, 083116.	3.3	10
77	Thermal stability study of Cr/Au contact formed on n-type Ga-polar GaN, N-polar GaN, and wet-etched N-polar GaN surfaces. Applied Surface Science, 2014, 317, 1-5.	6.1	2
78	Enhanced performance of dye co-sensitized solar cells by panchromatic light harvesting. Journal of the Korean Physical Society, 2014, 64, 904-909.	0.7	9
79	Temperature-dependent current–voltage characteristics of Er-silicide Schottky contacts to strained Si-on-insulator. Journal of Alloys and Compounds, 2013, 556, 252-258.	5.5	39
80	Two-step annealed CdS/CdSe co-sensitizers for quantum dot-sensitized solar cells. Current Applied Physics, 2013, 13, 1532-1536.	2.4	9
81	Post-annealing of CdS/ZnS-assembled TiO2 films for photoelectrochemical solar cells. Journal of the Korean Physical Society, 2013, 63, 2209-2214.	0.7	1
82	The Preparation and Photovoltaic Properties of Quasi-solid State Dye-Sensitized Solar Cells Containing Long Wavelength Absorbing Squaraine Dye. Molecular Crystals and Liquid Crystals, 2013, 581, 108-115.	0.9	0
83	Surface fermi level pinning of semipolar \$\$left({11ar 22} ight)\$\$ n-type GaN surfaces grown on m-plane sapphire substrates. Electronic Materials Letters, 2013, 9, 609-613.	2.2	7
84	Enhanced light harvesting of CdSe quantum dot sensitized bilayered ZnO nanostar/TiO2 nanotubes. Current Applied Physics, 2013, 13, S162-S167.	2.4	14
85	Bifunctional TiCl4 treatment in CdSe quantum dots sensitized TiO2 microrods for photoelectrochemical water splitting. Materials Letters, 2013, 111, 47-50.	2.6	9
86	Nanometer scale p-type Schottky barrier metal–oxide-semiconductor field-effect transistor using platinum silicidation through oxide technique combined with two-step annealing process. Journal of Alloys and Compounds, 2013, 563, 108-112.	5.5	0
87	Depinning of the Fermi level at the Ge Schottky interface through Se treatment. Scripta Materialia, 2013, 69, 809-811.	5.2	9
88	Enhanced Electrocatalytic Activity of the Annealed Cu _{2-x} S Counter Electrode for Quantum Dot-Sensitized Solar Cells. Journal of the Electrochemical Society, 2013, 160, H847-H851.	2.9	22
89	Morphological Control of Anodic TiO2 Nanotubes by the Modulation of Applied Potential. Chemistry Letters, 2013, 42, 758-760.	1.3	2
90	Influence of TiCl4Post-Treatment on TiO2Nanotube Arrays for Dye-Sensitized Solar Cells. Molecular Crystals and Liquid Crystals, 2012, 567, 19-27.	0.9	4

Kwang-Soon Ahn

#	Article	IF	CITATIONS
91	Carrier Transport Mechanism of a Low Resistance Ti/Al Ohmic Contact on (\$11ar{2}2\$) Semipolar n-Type GaN. Japanese Journal of Applied Physics, 2012, 51, 061001.	1.5	7
92	Effects of TiCl4Surface Treatment on Photoelectrochemical Response of TiO2Nanotube Arrays. Molecular Crystals and Liquid Crystals, 2012, 568, 192-197.	0.9	0
93	Carrier transport mechanism of Se/n-type Si Schottky diodes. Journal of Alloys and Compounds, 2012, 534, 37-41.	5.5	22
94	ZnS overlayer on in situ chemical bath deposited CdS quantum dot-assembled TiO2 films for quantum dot-sensitized solar cells. Current Applied Physics, 2012, 12, 1459-1464.	2.4	36
95	Effects of TiCl ₄ Treatment of Nanoporous TiO ₂ Films on Morphology, Light Harvesting, and Charge-Carrier Dynamics in Dye-Sensitized Solar Cells. Journal of Physical Chemistry C, 2012, 116, 21285-21290.	3.1	131
96	Conduction Mechanism of Se Schottky Contact to n-Type Ge. IEEE Electron Device Letters, 2012, 33, 949-951.	3.9	21
97	Effects of the flow rate of O2annealing ambient on structural and electrical properties of n+ emitter junctions formed using screen-printed phosphorus diffusion process. Surface and Interface Analysis, 2012, 44, 1440-1443.	1.8	0
98	Carrier Transport Mechanism of Ni/Ag/Pt Contacts to p-Type GaN. IEEE Transactions on Electron Devices, 2012, 59, 680-684.	3.0	19
99	Temperature-dependent current-voltage characteristics and reverse leakage conduction mechanism of Pt/n-type Si0.85Ge0.15 schottky rectifiers. Journal of the Korean Physical Society, 2012, 60, 1498-1503.	0.7	2
100	Schottky characteristics of Pt contacts on (11–22) semipolar n-type GaN grown on m-plane sapphire substrates. Electronic Materials Letters, 2012, 8, 17-20.	2.2	7
101	Transparent Zn-Doped In2O3Electrode Prepared by Radio Frequency Facing Target Sputtering for Flexible Dye-Sensitized Solar Cells. Molecular Crystals and Liquid Crystals, 2011, 538, 127-135.	0.9	4
102	Surface Properties of Poly(ethylene terephthalate) Films Modified by Inductively Coupled Plasma with Ar/N2Mixture Gases. Molecular Crystals and Liquid Crystals, 2011, 539, 210/[550]-217/[557].	0.9	4
103	Enhanced Photoelectrochemical Response of Graphene-Coated Al ₂ O ₃ -TiO ₂ Nanocomposite Photoanodes. Molecular Crystals and Liquid Crystals, 2011, 538, 272-277.	0.9	3
104	Improved Efficiency of Dye-Sensitized Solar Cell Using Graphene-Coated Al ₂ O ₃ -TiO ₂ Nanocomposite Photoanode. Molecular Crystals and Liquid Crystals, 2011, 538, 285-291.	0.9	12
105	Molecular Design and Photovoltaic Performances of Organic Dyes Containing Triphenylamine for Dye-Sensitized Solar Cell. Molecular Crystals and Liquid Crystals, 2011, 538, 278-284.	0.9	3
106	Enhanced electron lifetime in CdS quantum dot-sensitized solar cells with nanoporous-layer-covered TiO2 nanotube arrays. Journal of Applied Physics, 2011, 110, 054301.	2.5	17
107	Effects of anchoring groups in multi-anchoring organic dyes with thiophene bridge for dye-sensitized solar cells. Synthetic Metals, 2011, 161, 850-855.	3.9	59
108	Enhanced efficiency of dye-sensitized solar cells through TiCl4-treated, nanoporous-layer-covered TiO2 nanotube arrays. Journal of Power Sources, 2011, 196, 8904-8908.	7.8	58

Kwang-Soon Ahn

#	Article	IF	CITATIONS
109	CdS quantum dots grown by in situ chemical bath deposition for quantum dot-sensitized solar cells. Journal of Applied Physics, 2011, 110, 044313.	2.5	37
110	Synthesis and Photovoltaic Properties of Organic Photosensitizers Based on Phenothiazine Chromophore for Application of Dye-Sensitized Solar Cells. Molecular Crystals and Liquid Crystals, 2011, 538, 149-156.	0.9	7
111	Microstructural Evolution and Electrical Characteristics of Er-germanides Formed on Ge Substrate. Journal of the Electrochemical Society, 2011, 158, H751.	2.9	10
112	Effect of Conducting Ability of Electrolytes on the Photovoltaic Performance of Quasi-Solid State Dye-Sensitized Solar Cells. Molecular Crystals and Liquid Crystals, 2011, 538, 298-303.	0.9	0
113	<i>In-Situ</i> Transmission Electron Microscopy Investigation of the Interfacial Reaction between Er and SiO ₂ Films. Materials Transactions, 2010, 51, 793-798.	1.2	4
114	Two-dimensional dopant profiling in p+/n junctions using scanning electron microscope coupled with selective electrochemical etching. Electronic Materials Letters, 2010, 6, 55-58.	2.2	2
115	Effects of substrate temperature and RF power on the formation of aligned nanorods in ZnO thin films. Jom, 2010, 62, 25-30.	1.9	6
116	Effect of substrate temperature on the photoelectrochemical responses of Ga and N co-doped ZnO films. Journal of Materials Science, 2010, 45, 5218-5222.	3.7	17
117	Amorphous copper tungsten oxide with tunable band gaps. Journal of Applied Physics, 2010, 108, 043502.	2.5	14
118	Tri-Branched Tri-Anchoring Organic Dye for Visible Light-Responsive Dye-Sensitized Photoelectrochemical Water-Splitting Cells. Japanese Journal of Applied Physics, 2010, 49, 060219.	1.5	6
119	Temperature dependency and carrier transport mechanisms of Ti/p-type InP Schottky rectifiers. Journal of Alloys and Compounds, 2010, 504, 146-150.	5.5	85
120	CoAl2O4–Fe2O3 p-n nanocomposite electrodes for photoelectrochemical cells. Applied Physics Letters, 2009, 95, 022116.	3.3	32
121	Ternary cobalt spinel oxides for solar driven hydrogen production: Theory and experiment. Energy and Environmental Science, 2009, 2, 774.	30.8	60
122	(Photo)electrochemical Characterization of Doped ZnO Electrodes. ECS Meeting Abstracts, 2009, , .	0.0	0
123	Dye-sensitized solar cells employing non-volatile electrolytes based on oligomer solvent. Journal of Photochemistry and Photobiology A: Chemistry, 2008, 195, 198-204.	3.9	35
124	Carrier concentration tuning of bandgap-reduced p-type ZnO films by codoping of Cu and Ga for improving photoelectrochemical response. Journal of Applied Physics, 2008, 103, 073504.	2.5	65
125	Effects of a surfactant-templated nanoporous TiO2 interlayer on dye-sensitized solar cells. Journal of Applied Physics, 2007, 101, 084312.	2.5	56
126	Photoelectrochemical Properties of N-Incorporated ZnO Films Deposited by Reactive RF Magnetron Sputtering. Journal of the Electrochemical Society, 2007, 154, B956.	2.9	81

#	Article	IF	CITATIONS
127	Enhanced electron diffusion length of mesoporous TiO2 film by using Nb2O5 energy barrier for dye-sensitized solar cells. Applied Physics Letters, 2006, 89, 013103.	3.3	102